RSC Advances

Six new leads targeting Acetylcholinesterase as inhibitors
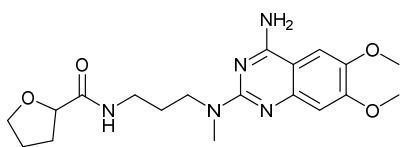
Alfuzosin
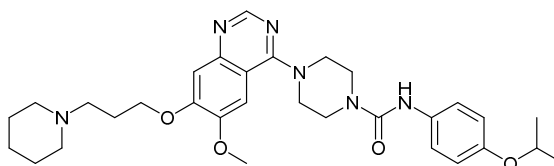
Tandutinib
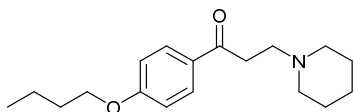
Dyclonine
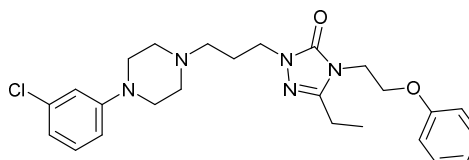
Nefazodone
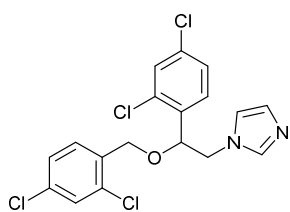
Miconazole
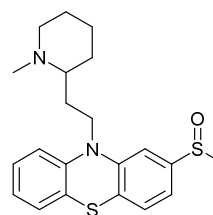
Mesoridazine

Journal Name

ARTICLE

Discovery of New Scaffolds from Approved Drugs as Acetylcholinesterase Inhibitors

Yao Chen, [a,d] Xiaoli Xu, [b,c] Tingming Fu, [a,d] Wei Li, [a,d] Zongliang Liu, [e,*] and Haopeng Sun [b,c,*]

Acetylcholinesterase inhibitors (AChEIs) is considered to be one of the most successful therapeutic strategies in the treatment of Alzheimer's disease (AD). To enlarge the scale of chemical scaffolds served as AChEIs, a compound collection containing 1280 approved drugs by U. S. food and drug administration (FDA) was screened. Six drugs, including **Alfuzosin**, **Tandutinib**, **Dyclonine**, **Nefazodone**, **Miconazole** and **Mesoridazine** exhibited potent inhibitory effect on acetylcholinesterase (AChE). The binding mode indicated their "dual site binding" manner, which targeted the catalytic site (CAS) and peripheral anionic site (PAS) simutaneously. Considering that approved drugs have proper physicochemical properties and good safety, these drugs provided us good starting point to further design selective and potent AChEIs with novel scaffold and good drug-like ability.

1. Introduction

Alzheimer's disease (AD) is the most common adult disease leading to impairment in memory, language skills, judgment and orientation.[1] Over 40 million people suffer from AD worldwide, and it accounts for nearly 70% of adult dementia.[2] It is considered that more and more people will suffer from this disease in the next several decades accompanied by the increase of the average age of people.[3] Therefore, effective therapeutic strategies are urgently needed. Although the exact etiology of AD is not completely understood so far, several common hallmarks, including cholinergic dysfunction,[4] amyloid-β (Aβ) deposits[5] and τ-protein aggregation[6] are considered to be tightly correlated to the pathophysiology and the progress of AD. Besides these factors, several other reasons such as stress condition,[7] neuroinflammation,[8] excitotoxicity,[9] calcium impairment,[10] mitochondrial dysfunction,[11] *et al*, are revealed to play important role in the development of AD. These factors provide deepening understanding of the mechanisms and novel insights into the therapeutic strategy of AD.

Although many active compounds with diverse mechanisms have been developed in the past decades, the main strategy for the treatment of AD in clinical is still to evaluate the level of acetylcholine (ACh) according to cholinergic hypothesis.[12] Five acetylcholinesterase inhibitors (AChEIs), named **tacrine**, **rivastigmine**, **galanthamine**, **donepezil** and **huperzine A** (Figure 1),

are approved to enter the market.[13] However, the effectiveness of these AChEIs has been proved to be palliative.[14] The drugs only offer limited and transient benefits and can not delay or prevent the progression of AD.[15] Considering that AD is a complicated and systematic disease, traditional agents that act only on one single target is not preferred in the treatment of AD.[16]
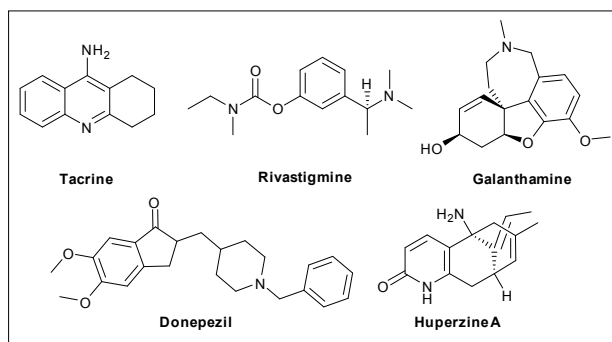
Figure 1. Approved agents for the treatment of AD.

In recent years, great efforts have been devoted to the discovery and development of "multi-target-directed ligands" (MTDLs)[17] of acetylcholinesterase (AChE), which bind simultaneously to both the catalytic anionic site (CAS) [18, 19] and the peripheral anionic site (PAS) [20, 21] of AChE. It is believed that such agents can supply greater affinity to AChE as well as multiple regulation effects in the treatment of AD. Based on this strategy, series of MTDLs AChEIs were designed, which showed promising anti-AD potential. Generally, MTDLs need multiple functional groups in order to modulate different targets simultaneously. This makes the scaffold of MTDLs usually complicated and highly hydrophobic, which reduced the druglikeness of the compounds. For example, many of MTDLs AChEIs exhibit high molecular weight and LogP, poor solubility, and are easily to be oxidized during the metabolic process,

---
[a.] School of Pharmacy, Nanjing University of Chinese Medicine, Nanjing, 210023, China.
[b.] Jiangsu Key Laboratory of Drug Design and Optimization, China Pharmaceutical University, Nanjing, 210009, China.
[c.] Department of Medicinal Chemistry, China Pharmaceutical University, Nanjing, 210009, China.
[d.] Jiangsu Collaborative Innovation Center of Chinese Medicinal Resources Industrialization
[e.] School of pharmacy, Yantai University, Yantai, 264005, China

which may cause potential problems in further development. Therefore, discovering potent structures with high druglikeness and ligand efficiency (LE) as starting point to design MTDLs AChEIs is an attractive and challenging task for medicinal chemists.

In the present study, we report our efforts in identifying chemical scaffolds for the design of MTDLs AChEIs. Considering that approved drugs usually have good physicochemical properties and safety, a compound collection containing 1280 drugs approved by food and drug administration (FDA) was screened for their AChE inhibitory effects. Six drugs, named **Alfuzosin**, **Tandutinib**, **Dyclonine**, **Nefazodone**, **Miconazole** and **Mesoridazine** were identified to function as AChEIs. The most potent compound **Alfuzosin** showed even comparable activity to **Donepezil**. The kinetic study as well as the binding mode analysis indicated these drugs acted as MTDLs. These scaffolds provide ideal templates for further design and optimization campaign in order to obtain highly potent and selective agents for the treatment of AD.

2. Results and discussion

2.1 Identification of six hits as AChEIs from FDA approved drugs.

A compound collection including 1280 FDA approved drugs were biologically screened following the Ellman's method[22] using Electrophorus electricus AChE (eeAChE) and BuChE from equine serum. Preliminary screening revealed 25 hits (data not reported) that exhibited over 50.0 % inhibitory activity on AChE. They were retained for further dose-dependent evaluation, while donepezil was used as positive control. Among all the hits, six compounds, named **Alfuzosin**, **Tandutinib**, **Dyclonine**, **Nefazodone**, **Miconazole** and **Mesoridazine** (Figure 2), showed potent and dose-dependently (Figure 3A) inhibitory activities on AChE, with IC_{50} around or below 1.0 μM (Table 1).
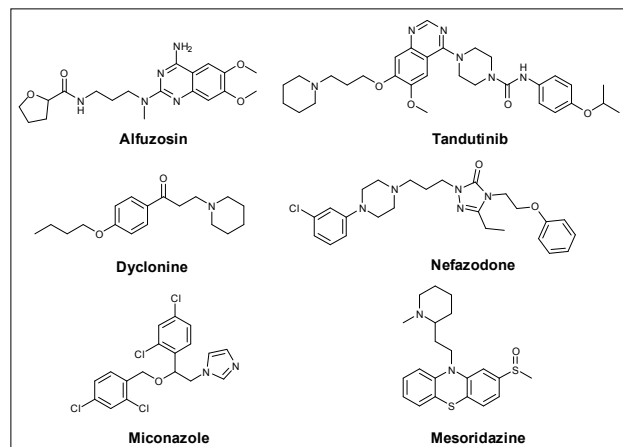

Figure 2. The structure of the six potent hits.

The most potent compound, **Alfuzosin**, exhibited comparable activity to **Donepezil** (0.018 ± 0.004 μM and 0.002 ± 0.0004 μM, respectively), indicating its potential in further structural optimization to achieve new scaffold as AChEIs. It also had similar molecular weight (MW) to Donepezil (389.46 and 379.50 respectively, Table 1).

To evaluate the selectivity of the hits on AChE, we tested the inhibitory effects (Figure 3B) of the hits on butyrocholinesterase (BuChE). To our delight, most of the compounds exhibited good selectivity on AChE except **Miconazole**, which showed better activity on BuChE (IC_{50} = 0.352 ± 0.071 μM, Table 1). **Alfuzosin**, **Dyclonine**, **Nefazodone and Mesoridazine** were totally not active on BuChE (IC_{50} > 100 μM, Table 1). Although **Tandutinib** showed moderate BuChE inhibitory effect, it was ten-fold less potent than its AChE activity. This high selectivity can avoid the peripheral side effect of the compounds in the treatment of AD. Therefore, they can serve as good leads for further structural optimization.
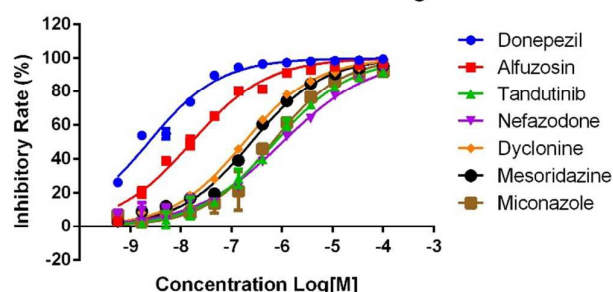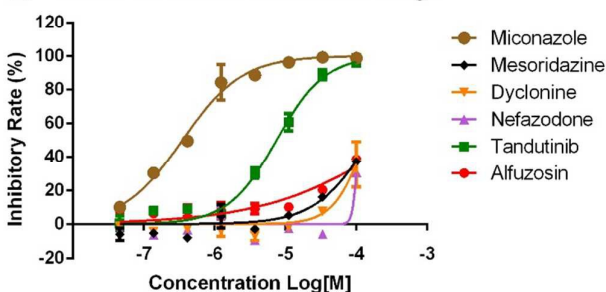
Figure 3. Inhibitory curve of the six hits on AChE and BuChE. The initial concentration was set as 100 μM and then 5 times dilution for another eleven concentrations. **Donepezil** was used as the positive control for AChE.

Table 1. The IC_{50} of the six hits on AChE and BuChE.

Compound	MW	AChE IC_{50} (μM)[a]	BuChE IC_{50} (μM)[a]
Alfuzosin	389.46	0.018 ± 0.004	> 100
Tandutinib	562.71	0.741 ± 0.149	7.494 ± 1.249
Dyclonine	289.42	0.181 ± 0.015	> 100
Nefazodone	470.01	1.037 ± 0.216	> 100
Miconazole	416.62	0.656 ± 0.164	0.352 ± 0.071
Mesoridazine	386.57	0.251 ± 0.034	> 100
Donepezil	379.50	0.002 ± 0.0004	ND

[a] The IC_{50} values of all the compounds were shown as Mean ± SE (n=3). For **Alfuzosin**, n=6.

2.2 Kinetics study

To gain more information on the mechanism of AChE inhibition, the kinetic studies for six hit compounds were further performed by using Lineweaver-Burk plots, which were reciprocal rates versus reciprocal substrate concentrations for

the different inhibitor concentrations resulting from the substrate-velocity curves for cholinesterases. [23]

For **Alfuzosin**, **Tandutinib**, **Nefazodone** and **Mesoridazine**, the Lineweaver-Burk plot showed both increased slopes (decreased Vmax) and intercepts (higher Km) at increasing concentrations of the inhibitors (Figure 4A, B, D and F), leading to a mixed-type inhibitory pattern. The data supported the

dual site (CAS and PAS) binding of the four compounds, indicating that they can serve as MTDLs AChEIs.

In contrast, a different plot type for **Dyclonine** and **Miconazole** was obtained. These two compounds showed constant Km and variant Vmax at different inhibitor concentrations, suggesting a non-competitive AChE inhibition. The data revealed that these two compounds may bind to a site different from the AChE substrate ACh.
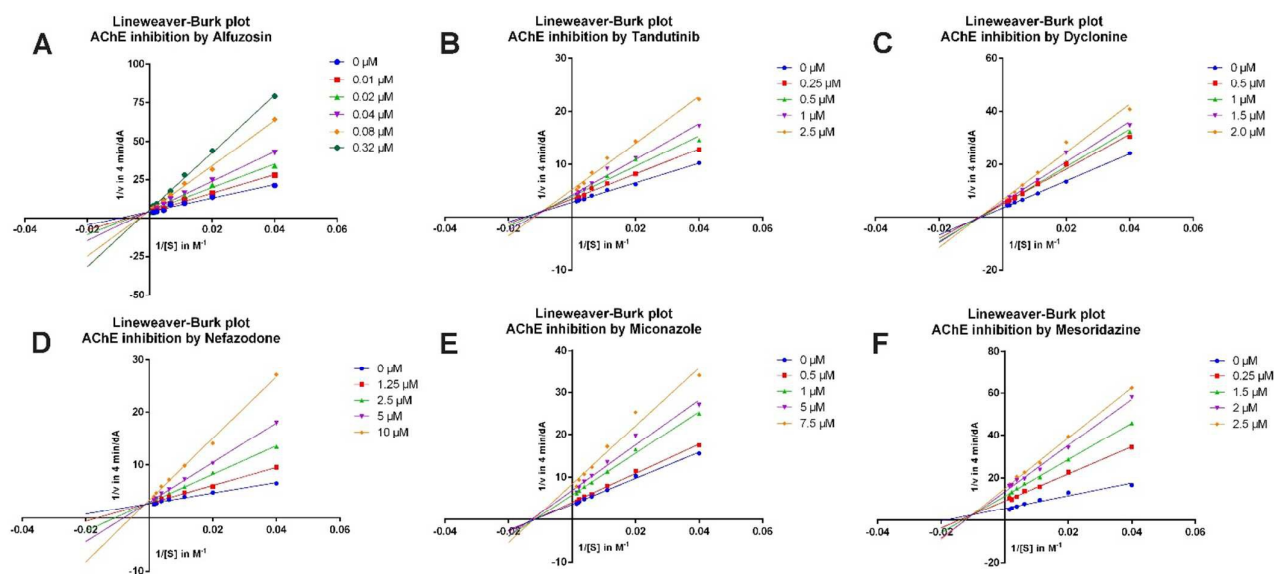

Figure 4. Lineweaver-Burk plots of **Alfuzosin** (A), **Tandutinib** (B), **Dyclonine** (C), **Nefazodone** (D), **Miconazole** (E) and **Mesoridazine** (F) resulting from subvelocity curves of AChE activity with different substrate concentrations (25–450 μM) in the absence and presence of the compounds with different concentrations.

2.3 Binding mode analysis of the six hits.

To support the data from kinetic study, molecular docking was performed for the six compounds to analyze their binding modes on AChE according to our previous study.[24] Based on the docking results, **Alfuzosin** exhibited an CAS and PAS dual site inhibitory manner on AChE. In detail (Figure 5A), the tetrahydrofuran ring of **Alfuzosin** bound to the CAS of AChE, forming strong hydrophobic contact to the side chain of Trp84 and His440. This occupation hindered the approach of ACh to the catalytic traid of AChE formed by Ser200, Glu327 and His440, leading to enzyme inhibition. The flexible linker of **Alfuzosin** bound to a narrow binding groove comprised of Asp72, Ser81 and Tyr121. The amide group can form proper contacts with the polar residues in this groove. The 4-amino quinazoline ring of **Alfuzosin** inserted into the PAS site of AChE including Tyr70, Trp279, Phe330 and Phe331, forming strong π-π stacking and hydrophobic contacts. The amino group interacted with Asp72 through a H-bond, which further improved the binding affinity. Therefore, this compound showed very potent inhibitory activity and consistent inhibitory pattern on AChE to that revealed by kinetic study. Based on the binding mode, we observed that the two methoxyl groups of **Alfuzosin**, which played an important role for the antihypertension effect, pointed to the outside solvent pocket of the protein, indicating the two methoxyl groups were not

necessary for the AChE binding. Therefore, removing or replacing them with other groups may enhance the target specificity.

For **Tandutinib**, it also formed CAS and PAS dual site binding mode (Figure 5B). The aniline group inserted into the CAS of AChE and interacted with Ser200 and His440, which can prohibit the catalysis of ACh by AChE. The piperazine group acted as the linker, which connecting the quinazoline ring functioned as PAS binding core, which contacted with Tyr70 and Try279 though π-π stacking interaction. However, according to the docking result, it seems that **Tandutinib** was too large compared to its binding pocket. Several groups, such as the isopropyl and piperidine ring, did not show any contribution to the binding affinity and made the binding pocket very crowded. To occupy the binding groove of AChE, **Tandutinib** need to form an unreasonable conformation, which reduced its binding affinity. This can explain its decreased activity compared to **Alfuzosin**. Therefore, replacing these groups by more simple substituents may improve the AChE inhibition.

Nefazodone (Figure 5D) formed similar binding pattern to **Tandutinib** and **Alfuzosin**. The chlorobenzene ring inserted into CAS of AChE. It formed halogen bond to His440 and hydrophobic interaction to Phe330 and Phe331, which stabilized its binding conformation. The triazol ring bounded to the PAS site though interacting with Tyr70 and Tyr334. However, we observed that the hydrophobic benzene at the terminal of **Nefazodone** pointed to the

outside of the protein near the solvent region. Replacement of this group with other hydrophilic chains might enhance the activity.

Mesoridazine (Figure 5F) bounded to CAS and PAS simultaneously. The tricyclic core contacted with Trp84 and Phe330 through π-π stacking and σ-π interaction. The N-methyl piperidine interacted with the side chain of His440. The sulfoxide group formed an H-bond with Ser124, which enhanced the binding affinity.

When **Dyclonine** and **Miconazole** were docked into the binding pocket of AChE, we observed different binding modes compared to the other four compounds mentioned above. Interestingly, the two compounds only located at the PAS of AChE. No group inserted into the CAS. This binding mode can support the non-competitive manner from kinetic study. We assumed that it was the length and the molecular shape of these two molecules caused such difference. Compared to the other four compounds, **Dyclonine** and **Miconazole** formed more shrink conformations, which made them could not

cover the CAS and PAS simultaneously. Additionally, the two compounds were highly hydrophobic, containing multiple aromatic rings or alky chains. This made them were prone to the more hydrophobic PAS of AChE.

In detail, the benzene ring of **Dyclonine** (Figure 5C) located at the pocket surrounded by Tyr121, Phe330 and Phe331. The oxygen atom and the carbonyl group formed two H-bonds with Tyr121 and Glu199, respectively, which locked the binding conformation at PAS. **Miconazole** (Figure 5E) interacted with the PAS mainly through the three aromatic rings. One dichlorobenzene ring contacted with Tyr70, Asp72 and Tyr121 through π-π stacking and cation-π interactions. The other dichlorobenzene ring contacted with Trp84 and Trp432. The imidazole ring also formed π-π stacking with Trp84. However, lacking of the polar intermolecular recognition might reduce the target specificity of this compound.
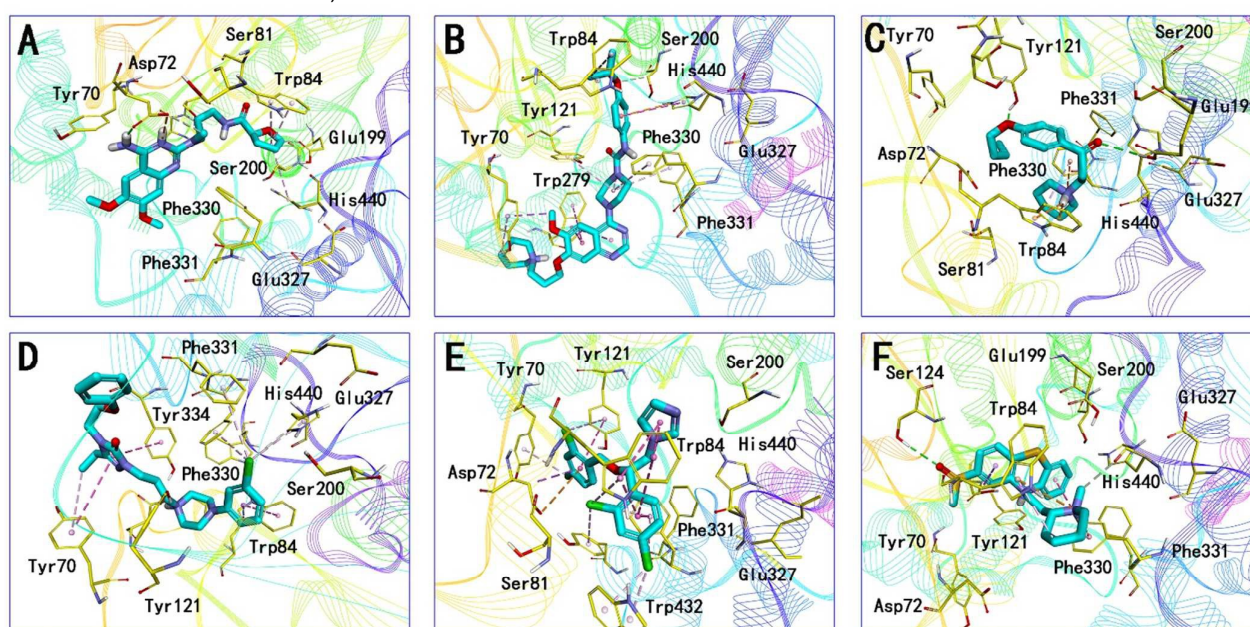

Figure 5. Binding mode prediction of **Alfuzosin** (A), **Tandutinib** (B), **Dyclonine** (C), **Nefazodone** (D), **Miconazole** (E) and **Mesoridazine** (F) with CAS of AChE (PDB id: 2CKM). Compounds were shown in blue stick mode, key residues were shown in yellow line mode. Hydrophobic contact   and   π-π   stacking   were   depicted   in   purple   dot   line,   H-bonds   were   in   green   dot   line.

3. Discussion.

Exploring active compounds among existing drug molecules is considered to be a lower-cost, lower-risk strategy for the discovery of new chemical entities. This is because approved drugs usually have confirmed properties, such as pharmacodynamics, pharmacokinetic, safety, based on a large scale of clinical study. Therefore, once an approved drug is revealed to be active in a new therapeutic area, it can be an ideal lead compound for further molecular design and optimization.

To have a deeply insight into the six hits, we analysed their drug-like ability by predicting some of the physicochemical properties, ADMET and toxicity potentials (Table 2). Firstly, all

the six compounds are predicted to have high Blood-Brain Barrier (BBB) penetration ability, indicating their potential usage for the AD treatment. **Alfuzosin** shows the best drug-like ability, including reasonable ClogP, pKa, solubility and cell permeability. But the compound has too many H-bond acceptors, leading to the high topological polar surface area (tPSA), which may limit its activity in the central system. Removing the methoxyl groups may solve this problem. **Alfuzosin** is predicted to have potential possibility in inducing carcinogenicity and teratogenicity. Therefore, structural modifications on the scaffold are necessary to avoid these potential toxicities. **Tandutinib**, **Nefazodone** and **Miconazole** have high ClogP (> 4.4), indicating a high lipophicity, which reduces the solubility of these compounds. High lipophilic compound usually has many problems in the metabolic

ARTICLE

process *in vivo*. Therefore, the three compounds have much higher ADMET risk compared to **Alfuzosin**, and are easily to be metabolized by CYP450 enzymes. **Dyclonine** and **Mesoridazine** have proper ClogP cell permeability, but the solubility is poor. All the hits except **Alfuzosin** are predicted to have hERG inhibition problem. And this is accordance with the fact that **Mesoridazine** was withdrawn from the United States market in 2004 due to irregular heart beat and QT-prolongation of the electrocardiogram (Table 3). Meanwhile, **Nefazodone** and **Miconazole** are predicted to have hepatotoxicity, and this prediction is supported by the fact that the sale of **Nefazodone** was discontinued in 2003 in some countries due to the rare incidence of hepatotoxicity (Table 3). Reducing the lipophicity and introducing proper groups to block the the metabolism on the aromatic rings of these compounds may be a rational strategy.

We summarized the original usage of the six drugs (Table 3). During the optimization process in an "old drug for new use" campaign, one of the most important challenges is to enhance the target selectivity, which is, improving the affinity on its new target, while reducing the activity on its original target. To achieve this goal, an efficient approach is to compare the pharmacophores of the compound on the new and original target. Removing pharmacophores that are not necessary for the new target, but are critical to the original target, can remarkably enhance the selectivity of the compound.

Introducing new pharmacophores, or replace the original pharmacophores based on the structure of the new target, can also be useful strategies.

According to the binding mode of the six drugs to AChE, the methoxy groups of **Alfuzosin**, which are important for the α_1-adrenoceptor inhibition, pointed to the outside solvent region of AChE. This mode may bring energy penalty when **Alfuzosin** binds to AChE. ADMET prediction also indicates that the two methoxy groups provide redundant H-bond acceptors. Therefore, the methoxy groups can be removed from the scaffold. π-π stacking to Trp84 of AChE is a common intermolecular interaction in the AChE inhibitors. To enhance the interaction, the tetrahydrofuran ring can be substituted by other aromatic rings. For **Tandutinib**, it is too large compared to the binding pocket of AChE. Some groups, such as isopropyl and piperidine ring, do not show any contribution to the binding affinity. Removing these groups can also reduce the lipophicity and help to solve the hERG inhibition problem. As mentioned above, **Nefazodone** and **Mesoridazine** have severe toxicity problems, which limit their clinical usage. Structurally, this may be originated from the triazole, piperidine or piperazine groups. Scaffold hopping to other rings may provide an efficient strategy to solve the problems.

Table 2. The physicochemical properties, ADMET and toxicity prediction of hits.

Properties	Alfuzosin	Tandutinib	Dyclonine	Nefazodone	Miconazole	Mesoridazine
ClogP	1.75	4.56	3.84	4.44	5.81	3.04
pKa	7.48, 0.92	11.39, 8.87, 4.56, 2.20	8.95	7.35, 2.24, 1.26	6.28	8.97, 1.18
Solubility[a]	2.98	2.33E-01	1.57E-01	8.27E-02	3.48E-03	9.40E-02
MDCK[b]	183.0	163.0	306.0	330.2	439.9	259.2
BBB penetration[c]	High	High	High	High	High	High
ADMET_Code[d]	HA	Sz, RB, HA, ch, ow, 3A	Vd, D6	Sz, RB, ow, fu, D6, 3A, ti	ow, Sw, fu, 1A, C9, 3A, ti	Vd
ADMET_Risk[f]	2.27	5.71	2.96	6.79	8.27	2.0
Toxicity[e]	Xr, Mu	hE	hE	hE, Xm, Mu, Hp	hE, SG, Hp	hE
Toxicity_Risk[f]	1.77	1.0	0.96	2.61	2.29	1.0
tPSA[g]	110.8	91.2	29.54	51.6	24.8	23.6

[a]Water solubility (mg/mL); [b]MDCK permeability (cm/s×10[7]); [c]Likelyhood of Blood-Brain Barrier penetration; [d]HA = H-bond acceptors, SZ = size, RB = rotatable bonds, ch = charge, ow = lipophilicity, 3A = CYP3A4, Vd = volume of distribution, D6 = CYP2D6, fu = fraction unbound, ti = inhibition of testosterone oxidation, 1A = CYP1A2, C9 = CYP2C9; [e]Xr = carcinogenicity in rat, Mu = Ames positive, hE = hERG inhibition, Xm = carcinogenicity in mice, SG = SGOT and SGPT evaluation, Hp = hepatotoxcity. [f]A score in the 0~24 range indicating the number of potential ADMET or Toxicity risk a compound might have. The higher the number is, the higher risk of a compound is; [g]tPSA = topological polar surface area.

Table 3. The original usage of the hits.

Compound	Usage summary and status
Alfuzosin[a]	An α_1-adrenoceptor antagonist that was launched in 1988 for the oral treatment of benign prostatic hyperplasia (BPH).
Tandutinib[a]	An inhibitor of the type III receptor tyrosine kinases for the treatment of glioblastoma and acute myeloid leukemia (AML). No recent developments have been reported.
Dyclonine[b]	An oral anaesthetic that is the active ingredient of Sucrets. It is also found in some varieties of the cepacol sore throat spray. It is used topically as the hydrochloride salt.
Nefazodone[b]	An antidepressant acts primarily as a potent antagonist at the 5-HT$_{2A}$ receptors.. Its sale was discontinued in 2003 in some countries due to the rare incidence of hepatotoxicity.
Miconazole[b]	An imidazole antifungal agent, commonly applied topically to the skin or to mucous membranes to cure fungal infections. It works by inhibiting the synthesis of ergosterol.
Mesoridazine[b]	A piperidine neuroleptic drug used in the treatment of schizophrenia. It was withdrawn from the United States market in 2004 due to irregular heart beat and QT-prolongation of the electrocardiogram.

[a]Information searching from Tomson Pharma Integrity; [b]Information searching from Wikipedia.

4. Conclusions

In conclusion, we identified six compounds, including Alfuzosin, **Tandutinib**, **Dyclonine**, **Nefazodone**, **Miconazole** and **Mesoridazine**, showed *in vitro* ChE inhibitory effects. Some of them, such as **Alfuzosin**, showed comparable AChE inhibitory activity to **Donepezil**. They provide new scaffolds for the design of potent and selective ChEIs. Most of them exhibited very high selectivity on AChE against BuChE, indicating their potential in avoiding the peripheral side effect in the treatment of AD. Additionally, as these compounds have already been or previously acted as drugs, their physicochemical properties as well as the safety can be assured for further development. Ideal lead compounds may be achieved after rational optimizations by medicinal chemists.

5. Experimental section

4.1 In vitro cholinesterase Inhibition Assay.

The assay followed the method of Ellman *et al.*, using a Thermo Scientific Varioskan Flash. AChE (C3389, Type VI-S, from Sigma) and BuChE (C0663, from human erythrocytes), 5,5'-dithiobis (2-nitrobenzoic acid) (Sigma reagent, DTNB, D218200), acetylthiocholine (ATC), and butyrylthiocholine (BTC) iodides were purchased from Sigma-Aldrich (Shanghai,

China). AChE/BuChE stock solution was prepared by adjusting 500 units of the enzyme and 1 mL of gelatin solution (1% in water) to 100 mL with water. This enzyme solution was further diluted before use to give 2.5 units/mL. ATC/BTC iodide solution (0.075 M) was prepared in water. DTNB solution (0.01 M) was prepared in water containing 0.15% (w/v) sodium bicarbonate. For buffer preparation, potassium dihydrogen phosphate (1.36 g, 10 mmol) was dissolved in 100 mL of water and adjusted with KOH to pH = 8.0 ± 0.1. Stock solutions of the test compounds were prepared in ethanol, 100 µL of which gave a final concentration of 10^{-4} M when diluted to the final volume of 132 µL. For each compound, a dilution series of at least five different concentrations (normally $10^{-4} \sim 10^{-9}$ M) were prepared.

For measurement, a cuvette containing 100 µL of phosphate buffer, 10 µL of the respective enzyme, and 10 µL of the test compound solution was allowed to stand for 5 min before 10 µL of DTNB were added. The reaction was started by addition of 2 µL of the substrate solution (ATC/BTC). The solution was mixed immediately, and exactly 2 min after substrate addition the absorption was measured at 25 °C at 412 nm. For the reference value, 10 µL of water replaced the test compound solution. For determining the blank value, additionally 10 µL of water replaced the enzyme solution. Each concentration was measured in triplicate at 25 °C. The inhibition curve was obtained by plotting percentage enzyme activity (100 % for the reference) versus logarithm of test compound concentration. Calculation of the IC$_{50}$ values was performed with GraphPad Prism 5.0.

4.2 Kinetic study

Kinetic measurements were performed in the same manner, while the substrate (ATC/BTC) was used in concentrations of 25, 50, 90, 150, 226, and 452 µM for each test compound concentration and the reaction was extended to 4 min before measurement of the absorption. Vmax and Km values of the Michaelis-Menten kinetics were calculated by nonlinear regression from substrate-velocity curves using GraphPad Prism 5.0. Linear regression was used for calculating the Lineweaver-Burk plots.

4.3 Molecular docking

The docking study was performed by CDOCKER module implemented in Discovery Studio 3.0. The principle of CDOCKER can be breifly summarized as follow: CDOCKER generates ligand "seeds" to populate the binding pocket. Each seed is then subjected to high temperature molecular dynamics (MD) using a modified version of CHARMm force field. The structure after MD run is then fully minimized under the forcefield. The solutions are then clustered according to position and conformation and ranked by energy. The cocrystal structure of Torpedo Californica AChE bound with bis(7)-tacrine (TcAChE, PDB id: 2CKM) was used for molecular docking. The binding sites were defined by residues around the CAS of AChE (in 6 Å radius). The heating step, cooling steps, and cooling temperature were set to 5000, 5000, and 310, respectively. Other parameters were kept as default.

4.4 Prediction of physicochemical properties.

Compound was firstly sketched using discovery studio 3.0 and then saved as sd format. It was then imported into ADMET predictor 7.0 (Simulation plus, USA) for ADMET and toxicity prediction. Calculation was performed under pH = 7.4. Other parameters were set as default. The results were exported into a sd file for further reading. The **t**opological polar surface area was predicted by Chemdraw 13.0.

4.5 Compound collection

All compounds were purchased from Topscience (http://www.tsbiochem.com/), with purity > 95.0 %.

Notes and references

1 C. Ballard, S. Gauthier, A. Corbett, C. Brayne, D. Aarsland, E. Jones, *Lancet*, 2011, **377**, 1019–1031.
2 C. Reitz, C. Brayne, R. Mayeux, *Nature Rev. Neurol.*, 2011, **7**, 137-152.
3 A. M. Palmer, *Trends Pharmacol. Sci.*, 2011, **32**, 141-147.
4 U. Holzgrabe, P. Kapková, V. Alptüzün, J. Scheiber, E. Kugelmann, *Expert Opin. Ther. Targets*, 2007, **11**, 161-179.
5 R. D. Terry, N. K. Gonatas, M. Weiss, *Ann. J. Pathol.*, 1964, **44**, 269-297.
6 I. Grundke-Iqbal, K. Iqbal, Y. C. Tung, M. Quinlan, H. M. Wisniewski, L. I. Binder, *Proc. Natl. Acad. Sci. U. S. A.*, 1986, **93**, 4913-4917.
7 M. Rosini, E. Simoni, A. Milelli, A. Minarini, C. Melchiorre, *J. Med. Chem.*, 2014, **57**, 2821-2831.
8 R. A. Linker, D. H. Lee, S. Ryan, A. M. van Dam, R. Conrad, P. Bista, W. Zeng, X. Hronowsky, A. Buko, S. Chollate, G. Ellrichmann, W. Bruck, K. Dawson, S. Goelz, S. Wiese, R. H. Scannevin, M. Lukashev, R. Gold, *Brain*, 2011, **134**, 678-692.
9 N. A. Kaidery, R. Banerjee, L. Yang, N. A. Smirnova, D. M. Hushpulian, K. T. Liby, C. R. Williams, M. Yamamoto, T. W. Kensler, R. R. Ratan, M. B. Sporn, M. F. Beal, I. G. Gazaryan, B. Thomas, *Antioxid. Redox Signaling* 2013, **18**, 139-157.
10 J. C. Diaz, O. Simakova, K. A. Jacobson, N. Arispe, H. B. Pollard, *Proc. Natl. Acad. Sci. U. S. A.*, 2009, **106**, 3348-3353.
11 G. Aliev, M. Priyadarshini, V. P. Reddy, N. H. Grieg, Y. Kaminsky, R. Cacabelos, G. M. Ashraf, N. R. Jabir, M. A. Kamal, V. N. Nikolenko, A. A. Zamyatnin, Jr.; V. V. Benberin, S. O. Bachurin, *Curr. Med. Chem.*, 2014, **21**, 2208-2217.
12 E. Scarpini, P. Scheltens, H. Feldman, *Lancet Neurol.*, 2003, **2**, 539–547.
13 D. Muñoz-Torrero, *Curr. Med. Chem.*, 2008, **15**, 2433-2455.
14 A. V. Jr. Terry, J. J. Buccafusco, *J. Pharmacol. Exp. Ther.*, 2003, **306**, 821-827.
15 Z. Luo, J. Sheng, Y. Sun, C. Lu, J. Yan, A. Liu, H. B. Luo, L. Huang, X. Li, *J. Med. Chem.*, 2013, **56**, 9089-9099.
16 A. Cavalli, M. L. Bolognesi, A. Minarini, M. Rosini, V. Tumiatti, M. Recanatini, C. Melchiorre, *J. Med. Chem.*, 2008, **51**, 347-372.
17 M. L. Bolognesi, R. Matera, A. Minarini, M. Rosini, C. Melchiorre, *Curr. Opin. Chem. Biol.*, 2009, **13**, 303-308.
18 J. L. Sussman, M. Harel, F. Frolow, C. Oefner, Goldman, I. Silman, *Science*, 1991, **253**, 872-879.
19 P. H. Axelsen, M. Harel, I. Silman, J. L Sussman, *Protein Sci.*, 1994, **3**, 188-197.
20 P. Muñoz-Ruiz, L.; Rubio, E. García-Palomero, I. Dorronsoro, M. del Monte-Millán, R. Valenzuela, P. Usán, C. de Austria, M. Bartolini, V. Andrisano, A. Bidon-Chanal, M. Orozco, F. J. Luque, M. Medina, A. Martínez, *J. Med. Chem.*, 2005, **48**, 7223-7233.
21 Y. Bourne, P. Taylor, Z. Radić, P. Marchot, *EMBO J.*, 2003, **22**, 1-12.
22 G. L. Ellman, K. D. Courtney, V., Jr. Andres, R. M. Feather-Stone, *Biochem. Pharmacol.*, 1961, **7**, 88-95.
23 Y. Chen, J. F. Sun, L. Fang, M. Liu, S. X. Peng, H. Liao, J. Lehmann, Y. H. Zhang, *J. Med. Chem.*, 2012, **55**, 4309-4321.
24 Y. Chen, Z. L. Liu, T. M. Fu, W. Li, X. L. Xu, H. P. Sun, *Bioorg. Med. Chem. Lett.*, 2015, **25**, 3442-3446.

RSC Advances Accepted Manuscript